Nigerian Research Journal of Engineering and Environmental Sciences 6(2) 2021 pp. 554-560
p ISSN: 2635-3342; e ISSN: 2635-3350

Nigerian Research Journal of Engineering and Environmental Sciences
Journal homepage: www.rjees.com

Original Research Article

Effects of Iron-Millscale Addition on the Electrical and Thermal Properties of Aluminum-Nickel Alloy

***[1]Sekunowo, O.I., [1]Uwandu, A.C. and [2]Obasa, D.V.**

[1]Department of Metallurgical and Materials Engineering, Faculty of Engineering, University of Lagos, Lagos State, Nigeria.
[2]Department of Mechanical Engineering, Edo State University, Uzairue, Edo State, Nigeria.
*osekunowo@unilag.edu.ng

http://doi.org/10.5281/zenodo.5805154

ARTICLE INFORMATION

Article history:
Received 11 Nov 2021
Revised 01 Dec 2021
Accepted 09 Dec 2021
Available online 30 Dec 2021

Keywords:
Aluminium-nickel alloy
Electrical resistivity
Iron-millscale
Heating-element
Thermal stability

ABSTRACT

Most alloys employed in the fabrication of metal-based heating elements are known to be plagued by low hot strength and debilitating embrittlement resulting in epileptic performance. In this study, electrical resistivity and thermal characteristics of iron-millscale (IMS) modified aluminium-nickel alloy were assessed for heating element application. The alloy was synthesised by adding varied IMS particles to the base aluminium-nickel mixture and cast in metal moulds. Cast samples were characterised for electrical resistivity, thermal stability and microstructural integrity using appropriate state of the art tools. The results showed that among the varied IMS additions, the 4 wt. % IMS particle samples exhibited the best performance in terms of thermal stability (345 °C), electrical resistivity (47.1-52.3 Ωm) under applied current in the range of 10-50 A. Contributions to these levels of properties enhancement stem from the inducement of quasi ferritic AlNiFe precipitates within the matrix.

1. INTRODUCTION

The dearth of energy infrastructure for research and domestic applications has continued to limit output of researchers and also hampered improved standard of living in most developing countries (Gaal and Afrah, 2017). In this context, the role of high quality heating element in thermal processing such as heat treatment, roasting and drying cannot be over emphasised. According to David *et al* (2003), the sophistry of most modern devices has further thrown up a wide area of need for quality heating elements. These include LED (light emitting diode) screens, Wi-Fi control, smart meters, digital keypads and programmers requiring varying temperature heating cycles (Shin *et al*., 20016; Hallur *et al*., 2017; Kumbhar and Sonage 2018).

However, available conventional heating elements are both expensive and plagued by a relatively low thermal stability (Molina *et al.*, 2011; Ronald and Harvey, 2011; Zaitizila *et al.*, 2018). To overcome these limitations, efforts are being directed towards the development of heating elements with engineered structures that confer improved thermal characteristics using new materials at competitive cost.

Most metal-based heating element materials including nickel-chromium alloy possess austenitic microstructure. Such materials tend to exhibit relatively low resistance to oxidation at elevated temperature (Sabioni *et al.*, 2003; Wang *et al.*, 2020). For example, iron-chromium-aluminium (FeCrAl) alloys have been traditionally used as heating elements and critical heating components in temperature furnaces/reactors due to their superior oxidation resistance. A rather high oxidation at operating temperatures is the precursor of critical function impairment of heating elements (Raduta *et al.*, 2016). This accounts for the undesirable hot-strength often demonstrated by austenitic heating element components. It is established that ferritic heating elements offer higher resistant to oxidation at elevated temperatures coupled with better stability in strength (Wang *et al.*, 2020). The addition of varied percent of iron and its derivative is known to aid the microstructural transformation in the body centred cubic (BCC) phase in preference to face centred cubic (FCC) structure (Satyanarayana and Pandey, 1995; Ou, 2017; Meiser and Urbassek, 2019). In addition, the BCC matrix is adjudged to confer longer service life on metal-based heating elements (Ersoy *et al.*, 2002; Molina *et al.*, 2011). Therefore, heating element devices such as oil baths, salt and sand bathes, heat guns and hot plates require functional composition modification for improved and efficient functionality.

Iron-millscale (IMS) is basically a generic iron oxide (Fe_xO; where x takes the value from 1-3). It usually forms in the form of flaky scale on steel billets during re-heating prior to hot rolling. The material is regarded as a waste resulting in low yield during hot rolling of steel. Acumination of the waste on the shop floor often poses a great safe disposal challenge to steel millers. However, iron-millscale is considered a rich iron source with minimum impurities (Chokschi *et al.*, 2018; Bugdayci *et al.*, 2018). In addition, IMS has a propensity to initiate the nucleation of ferritic structure in most aluminium-based alloys (Wang *et al.*, 2021). In view of the foregoing, the use of emerging engineering materials should be encouraged in the fabrication of heating element to reduce cost, engender value addition and promote cleaner environment. Thus, the focus of the current work was to employ IMS particles to modify the microstructure of aluminium-nickel alloy with a view of enhancing its electrical and thermal properties suitable for application as heating element.

2. MATERIALS AND METHODS

2.1. Materials Preparation

The main materials employed in the work include aluminium ingots (Figure 1a) obtained from the Nigerian Aluminium Extrusion (NIGALEX) Company located in Oshodi, Lagos, Nigeria, Nickel billet (Figure 1b) which was sourced commercially and iron-millscale (Figure 1c) which was supplied by African Steel Mills located in Ikorodu, Lagos State, Nigeria. Preparations of the materials involved briquetting of the aluminium ingots after slicing into smaller pieces. After that, the nickel billet was mounted on a lathe to obtain nickel fillings by grinding while iron-millscale (IMS) was oven dried for 3 h, then ball milled and sieved into 106 µm particles. All these procedures were carried out to facilitate ease of materials design as shown in Table 1.

(a) (b) (c)

Figure 1: Materials (a) Aluminium ingot (b) Nickel billet (c) IMS particles, 106 µm

Table 1: Materials design

Sample ID	Alloy mixture (wt. %)		
	Aluminium	Nickel	Iron-millscale
A_0	98	2	0
A_2	94	4	2
A_4	90	6	4
A_6	86	8	6

2.2. Charging, Melting and Casting

The materials were charged into a crucible furnace according to the varied proportions of each element as shown in Table 1. Charging was carried out in sequence with nickel fillings and IMS charged first and both preheated to 500 ^oC. This was followed by charging of the appropriate weight percent of aluminium briquettes while the furnace temperature was raised to 700 ^oC. The molten melt was stirred using a long metal rod, homogenised at 750 ^oC and cast into cylindrical die moulds. Five samples were cast from each alloy formulation and all the samples were annealed in a muffle furnace at 350 ^oC for 2 h in preparation for characterisation.

2.3. Material Characterisation

Prior to the charging of materials into the muffle furnace, elemental composition analysis was carried out on nickel using a metal analyser (model, ARL 3460B, Switzerland) while X-Ray fluorescent (XRF), (PerkinElmer 2020, USA) composition analysis was conducted on the IMS particles. The cast samples were also subjected to microstructural integrity analysis using both optical microscope (OM) and scanning electron microscopy (SEM) coupled with energy dispersive spectroscopy (EDS). The samples electrical resistivity regime was evaluated at varied current, 10-400 amps and 230 V. The alloys thermal stability regime was evaluated through thermal gravimetric analysis (TGA) coupled with derivative thermogravimetry (DTG) using PerkinElmer thermal analyser. This method of characterisation was employed because the fabricated alloys are composed mainly of aluminium as matrix with minor addition of IMS particles. Therefore, it is safe to consider the alloys as composites (Zaitizila *et al*., 2018).

3. RESULTS AND DISCUSSION

3.1. Elemental Composition of Materials

Results of the spectrochemical analysis on nickel and XRF of IMS are presented in Tables 2 and 3 respectively. Materials elemental composition analysis provides the necessary information that determines the various phase transformations possible during their synthesis. These phases often correlate the microstructures that are induced in the material which eventually determine critical physical properties (Meiser and Urbassek, 2019). From the composition analysis results on nickel as shown in Tables 2a and 2b, the relatively significant presence of refractory compounds including CaO, TiO_2, BaO and Cr_2O_3 suggests the possibility of achieving ferritic phase transformation according to Ugheoke *et al* (2013) and Okamoto *et al* (2016). Most of the compounds and elements are seen to be present in the XRF analysis result on IMS (Table 3). This underscores the need for an informed material selection practice in alloy development.

Table 2a: Elemental composition of nickel by spectrochemical analysis

Element	Si	S	Fe	Co	Ni	Cu
Wt. %	0.118	0.151	0.024	0.053	99.417	0.237

Table 2b: composition of nickel by XRF analysis

Element	Fe_2O_3	CaO	BaO	TiO_2	NiO	Cr_2O_3
Wt. %	3.538	1.141	0.457	0.242	94.506	0.237

Table 3: XRF composition analysis of IMS

Compounds	FeO	Fe_2O_3	Fe_3O_4	SiO_2	MgO	CaO	MnO
Wt. %	67.806	28.738	6.186	0.011	0.015	0.221	0.023

3.2. Microstructure

The alloys microstructural features were obtained using both optical microscopy and scanning electron microscopy coupled with energy dispersive spectroscopy. Using an OM, the microstructural features obtained at 0 wt. % and 4 wt. % IMS addition are shown in Figure 2a and 2b respectively. It should be noted that the choice of 0 wt. % and 4 wt. % was borne out of the need to showcase the differences between the alloy microstructures developed at zero and 4 wt. % IMS addition. Thus, SEM/EDS tools were employed to further X-rayed the 4 wt. % IMS addition sample microstructure (Figure 2c) and the elemental spectrograph (Figure 2d). Homogeneous dispersion of complex aluminium-nickel (AlNi) precipitates is seen within the aluminium matrix (Figure 2a).

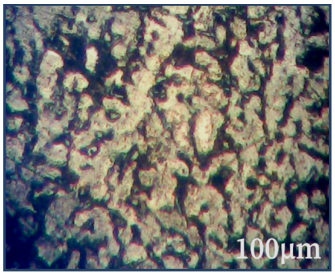

(a)

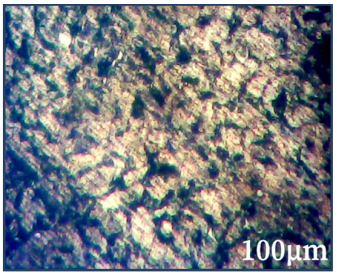

(b)

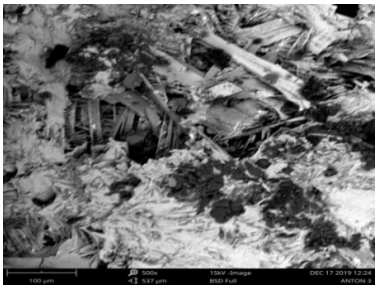

(c)

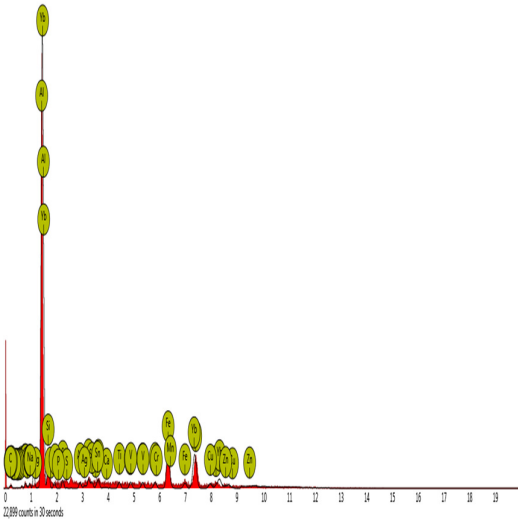

(d)

Element number	Element symbol	Element name	Atomic conc.	Weight conc.
13	Al	Aluminium	47.50	32.84
28	Ni	Nickel	15.74	23.67
26	Fe	Iron	10.61	15.19
29	Cu	Copper	3.01	4.90
30	Zn	Zinc	2.89	4.84
14	Si	Silicon	4.30	3.10
50	Sn	Tin	0.82	2.50
47	Ag	Silver	0.68	1.89
25	Mn	Manganese	1.32	1.87
6	C	Carbon	5.51	1.70
24	Cr	Chromium	0.90	1.20
22	Ti	Titanium	0.90	1.10
20	Ca	Calcium	1.05	1.08
19	K	Potassium	1.06	1.06
23	V	Vanadium	0.75	0.98
16	S	Sulfur	0.87	0.72
11	Na	Sodium	0.86	0.50
15	P	Phosphorus	0.61	0.49
12	Mg	Magnesium	0.61	0.38

(e)

Figure 2: Micrographs / Spectrograph: (a) OM of 0 wt. % IMS (b) OM of 4 wt. % IMS (c) SEM of 4 wt. % IMS (d) EDS of 4 wt. % IMS addition

The precipitates appear coalesced with a preferred orientation which may predispose the alloy to undesirable mechanical properties. Although similar microstructural features were induced in the alloy at 4 wt. % IMS particles addition as presented in Figure 2b, however, the composition of the precipitates is predominantly aluminium-nickel-iron (AlNiFe) which is quite different from AlNi. This was revealed in the sample's EDS spectral (Figure 2d). The ferritic AlNiFe structure is essentially similar to the FeCrAl precipitates developed in the works of Satyanarayana and Pandey (1995) and Sabioni *et al.* (2003) and recently the work of Kelvin

et al. (2017). In agreement with Meiser and Urbassek (2019) and Wang *et al.* (2020), this microstructure is known to offer higher resistance to oxidation at elevated temperatures coupled with better stability in strength.

3.3. Thermal Stability Regime

The combination of TGA/DTG tool was employed to measure the alloy thermal stability regime as the material weight changes upon heating until the mass becomes stable. Preliminary characterisation on the alloy formulations showed that the thermal performances of the 2 wt. % and 6 wt. % IMS addition were abysmally poor. This may be attributed to the inducement of incoherent precipitates within their matrices thereby rendering the samples inconsequential for presentation. This formed the basis of focus on 0 wt. % and 4 wt. % IMS addition samples. TGA was therefore conducted on 18.26 mg of the 4 wt. % IMS addition sample being the formulation that demonstrated the best relevant thermal characteristics. Figure 3 shows the plot of the thermal curve (red) exhibiting an onset monotonous weight-loss at 97%. By subjecting the sample to a temperature range of 46 - 663 ^{o}C at 10 ^{o}C/min heating rate, the derivative peak temperature (T_p) occurred around 345 ^{o}C corresponding to -3.15 %/min. This is the point of greatest rate of change on the weight-loss curve. Beyond this temperature, the sample begins to deteriorate having suffered about 68% mass loss. The structure modifying influence promotes development of ferritic intermetallic which improved thermal stability of the alloy in agreement with the report of Ugheoke *et al.* (2013), Zaitizila *et al.* (2018) and Sekunowo *et al.* (2019). Finally, the mass loss became stable at 610 ^{o}C.

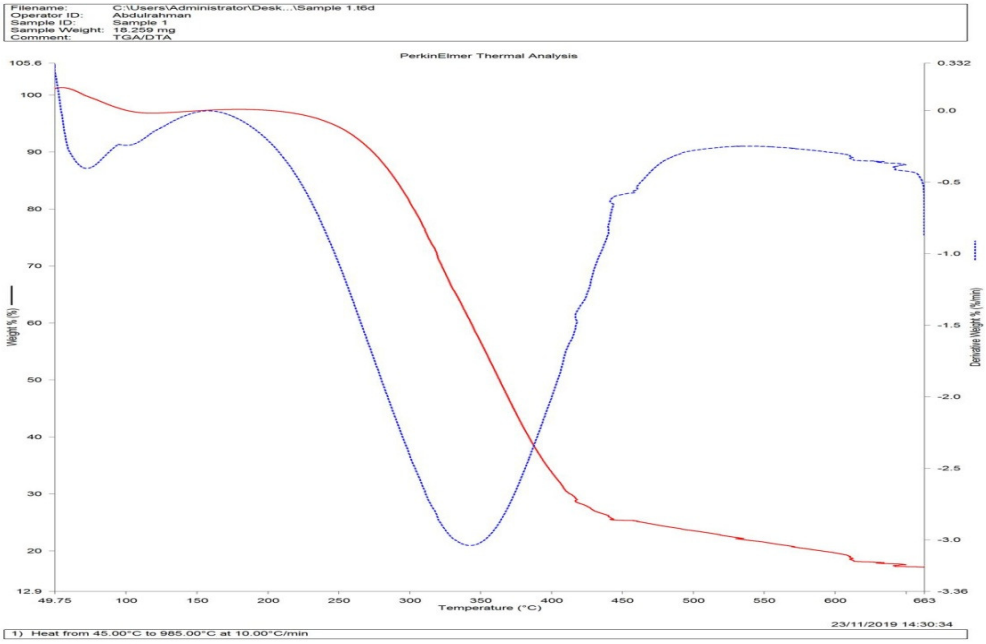

Figure 3: TGA/DTG curves at 4 wt. % IMS addition

3.4. Electrical Resistivity

The alloys propensity to resist free flow of electric current was evaluated at varied electric current from 10-400 A. The results which are illustrated in Figure 4 show that the 6 wt. % IMS addition sample gave the highest electrical resistivity of 65.4 Ωm when 10 A was applied. As the applied current increased, there was a significant drop in the specific resistance exhibited by samples A_0, A_2 and A_6 while sample A_4 recorded only a marginal reduction in resistivity values. In all, sample A_4 demonstrated a stable electrical resistivity regime which is between 48.6 Ωm and 55.0 Ωm for the current spectrum of 10-400 A. This appears to agree with Sekunowo *et al* (2019). The range of current peculiar to most common heating element such as electric

kettle, pressing iron, boiling-ring, etc., is between 10 A and 50 A. According to Dryden (2013) and Zhao *et al.* (2020), it is expected that a candidate material for heat element application should offer sufficient level of resistance to current flow thereby inducing desirable amount of heat energy. The 4 wt. % IMS alloy best approximates the electrical resistivity regime as it compared well with the conventional cupronickel alloys used as heating element.

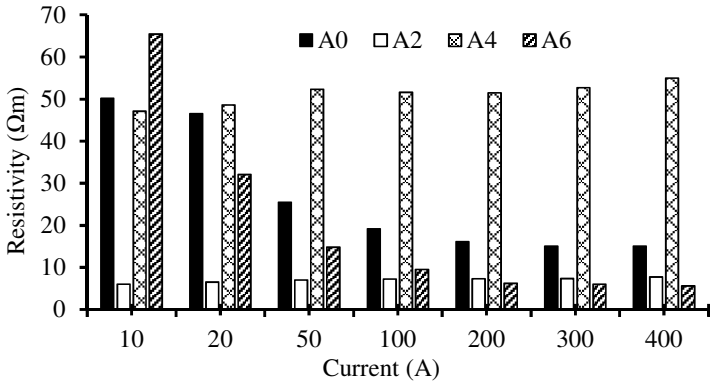

Figure 4: Electrical resistivity of samples at varied applied electric current

4. CONCLUSION

Iron-millscale-modified aluminium-nickel alloy has been successfully fabricated and characterised for heating element application. The 4 wt. % IMS formulation exhibited thermal and electrical properties employed as heating elements. This development is attributable to the inducement of quasi ferritic AlNiFe precipitates within the matrix. The alloy upper useful temperature was 345 ^{o}C while the mass was observed to be thermally stable around 610 ^{o}C. The electrical resistivity of 47.1-52.3 Ωm at impressed current from 10-50 A appear sufficient for producing desirable heat energy in the material. Given these levels of performances, the developed alloy can be recommended for use as heating element in electric kettle, pressing iron and boiling ring. The overall contributions of this study include value addition coupled with enhanced environmental cleanliness for the conversion and utilisation of iron-millscale waste.

5. CONFLICT OF INTEREST

There is no conflict of interest associated with this work.

REFERENCES

Bugdayci, M., Alkan, M., Turan, A. and Yuceil, K. (2018). Production of Iron Based Alloys from Mill Scale through Metallothermic Reduction. *High Temperature Materials and Processes*, 37(9-10), pp. 88-98.

Chokschi, Y., Sompura, N. and Dutta, S. K. (2018). Utilization of Steel Plants Waste. *Material Science & Engineering International Journal,* 2(5), pp. 144-147.

David, J., Eve, B. and Fred, E. (2003). *Heat Generating Kitchen Appliances*. Encyclopaedia of Modern Everyday Inventions, Greenwood Publishing Group, USA.

Dryden, I. G. (2013). *Electrical Heating Fundamentals.* Second Edition, Butterworth-Heinemann Publshers, Ohio, USA.

Ersoy, N., Wang, L. and Shatil, G. (2002). A Case Study of the Failure of an Electric Heater by Thermal Fatigue. *Proceedings of the 8th International Fatigue Conference, Stockholm, Sweden,* 1, pp. 12-21.

Gaal, H. O. and Afrah, N. A. (2017). Lack of Infrastructure: The Impact on Economic Development as a case of Benadir Region and Hir-shabelle, Somalia, *Developing Country Studies,* 7(1), pp. 49-55.

Hallur, S., Kulkarni, R. and Patavardhan, P. (2017). Smart Components for a Smart Energy Meter. *International Journal of Advance Research in Engineering, Science & Technology*, 4(3), pp. 544-565.

Kevin, G., Mary, A., Yukinori, Y. and Kurt, A. (2017). *Handbook of Material Properties of FeCrAl Alloys for Nuclear Power Production Applications*. Nuclear Technology Research and Development. Oak Ridge & Brookhaven: National Laboratory, USA.

Kumbhar, S. and Sonage, B. (2018). Enhancement of Thermal Efficiency and Cost Effectiveness by Development of Melting Furnace by Revamping and Troubleshooting Fuel-fired Furnace. *Heat Transfer-Asian Research*, 48, pp. 164-181.

Meiser, J. and Urbassek, S. (2019). Effect of Alloying Elements on the α-γ Phase Transformation in Iron. *Materials,* 12, pp. 55-66.

Molina, R., Amalberto, P. and Rosso, M. (2011). Mechanical Characterization of Aluminium Alloys for High Temperature Applications Part 2: Al-Cu, Al-Mg Alloys. *Metallurgical Science and Technology,* 29(2), pp. 5-24.

Okamoto, H., Schlesinger, M. and Mueller, E. (2016). *Alloy Phase Diagrams*. ASM Handbook, 3, pp. 2-14.

Ou, X. (2017). Molecular Dynamics Simulations of FCC-to-BCC Transformation in Pure Iron: A Review. *Materials Science and Technology*, 33(7), pp. 822-835.

Raduta, A., Nicoara, M., Cucuruz, L. and Locovei, C. (2016). Optimal Design of Heating Elements Sheathed with INCOLOY Super-alloy 800. *Applied and Theoretical Mechanics*, 3(5), pp. 208-220.

Ronald, N. and Harvey, S. (2011), The Mayer-Joule Principle: The Foundation of the First Law of Thermodynamics. *The Physics Teacher*, 49, pp. 484-487.

Sabioni, A., Huntz, A., Luz, E., Mantel, M. and Haut, C. (2003). Comparative Study of High Temperature Oxidation Behaviour in AISI 304 and AISI 439 Stainless Steels. *Materials Research*, 6(2), pp. 179-185.

Satyanarayana, D. and Pandey, M. (1995). The Role of Active Elements in Fe-Cr-AI Alloys for Heating Element Applications. *Indian Defence Metallurgical Research Laboratory*, 18(3), pp. 207-221.

Sekunowo, O., Durowaye, S. and Fashakin, G. (2019). Electrical and Thermal Characterisation of Millscale Modified *Sn-Cu* Lead-Free Solders. *Journal of the Institute of Engineering*, Tribhuvan University, Nepal, 15(1), pp. 38-47.

Shin, Y., Ahn, S. and Kim, C. (2016). Performance Characteristics of PTC Elements for an Electric Vehicle Heating System. *Energies*, 9, pp. 813-912.

Ugheoke, B., Mamat, O. and Ari-Wehjoedi, B. (2013). Thermal Expansion Behaviour, Phase Transitions and some Physico-mechanical Characteristics of Fired Doped Rice Husk Silica Refractory. *Journal of Advanced Ceramics*, 2(1), pp. 79-86.

Wang, S., Zheng, Z., Zheng, K., Long, J., Wang, J., Ren, Y. and Li, Y. (2020). High Temperature Oxidation Behaviour of Heat Resistant Steel with Rare Earth Element Ce. *Materials Research Express*, 7(1), pp. 4-16.

Wang, X., Jiang, J., Li, G., Shao, W. and Zhen, L. (2021). Particle-Stimulated Nucleation and Recrystallization Texture Initiated by Coarsened Al2CuLi Phase in Al-Cu-Li Alloy. *Journal of Materials Research and Technology,* 10, pp. 643-650.

Zaitizila, I., Halimah, M., Muhammad, F. and Faznny, M. (2018). Thermal Stability and Effect of Heat Treatment on Manganese Doped Silica Borotellurite Glass. *Journal of Materials Science and Chemical Engineering*, 6, pp. 24-30.

Zhao, H., Yan, N., Xing, Z., Chem, L. and Jiang, L. (2020). Thermal Calculation and Experimental Investigation of Electric Heating and Solid Thermal Storage System. *Energies,* 13, pp. 41-60.